Journal of Engineering and Applied Sciences 2 (4): 706-713, 2007

Comparative Study by EIS on the Corrosion Resistance of Electroplated Zn Coating in Different Corrosive Media

[1]Y. Hamlaoui, F. [2]Pedraza-Diaz and [3]L. Tifouti
[1]Centre Universitaire de Souk-Ahras, BP 1553 Souk-Ahars 41000, Algérie
[2]Laboratoire d'Etudes des Matériaux en Milieux Agressifs LEMMA,
Université de la Rochelle, 17042 La Rochelle Cedex1, France
[3]Laboratoire Génie d'Environnement, Université Badji Mokhtar,
BP 1223 El Hadjar Annaba, Algérie

Abstract: In this research, corrosion monitoring of Zn-based coatings is investigated through potentiodynamic, immersion and Electrochemical Impedance Spectroscopy (EIS) methods. This study is devoted to the study focuses on the corrosion resistance of a laboratory-made electrolytic coating. For such purpose, the corrosion behaviour is studied in different media (NaCl, NaOH and rain water), at different concentrations and varying pH and oxygen concentration. The results show that EIS allows to establish the interfacial reactions and the dissolution mechanisms occurring in three corrosive media, hence to foresee the protection conferred by these coatings. The kinetic model describing the Zn dissolution in aereted NaCl and Na_2SO_4 solutions, proposed in the literature, applies partially in the case of galvanised steel. Finally, each Zn/medium interface is characterised by a specific equivalent circuit giving a similar impedance response. It is concluded that EIS appears as a quick and reliable technique to evaluate the corrosion resistance of industrial coatings depending on the medium considered.

Key words: Electrochemical impedance spectroscopy, zinc, galvanised steel, corrosion

INTRODUCTION

Due to the susceptibility of steel to corrosion, it is always used with a protective coating. Zinc is use full, especially when it is used in the form of a thin coating. Hot-dip galvanising is the most widely used process to apply metallic coatings. More recently, the assessment of corrosion behaviour by EIS on industrial Zn-based coatings has been addressed on a 0.5 M sulphate medium (Cachet *et al*., 2002). It was concluded that the electrolytic and the hot-dip Zn coatings were less sensitive to corrosion probably due to the initial presence of impurities in the metal substrate. With an aim of having well controlled thickness, uniform surfaces and without imperfections, in fact always recourse to electrolytic coatings. Contrary to hot galvanising, when applied by electroplating, the coating is pure zinc. Surface analysis of electroplated zinc steel gives evidence that the surface after air exposure is always oxidized by a zinc oxide layer to a depth of more than 100A°(Leroy and Schmitz, 1988). Recently Zhang *et al*. (2005) used the electrochemical noise to study the zinc electrodeposition process. The author showed that when the electroplating current density decrease, the electrocrystallisation reaction will change from diffusion control through mixed control to electrochemical polarisation control. The same phenomenon was observed with the increase of Zn^{+2} concentration. Moreover, the zinc electrocrystallisation often leads to irregular and no compact deposits and the morphology of zinc deposits will change from spongy through compact to dentritic with the increase of electroplating current density (Blanc *et al*., 1978). Corrosion monitoring is typically carried out using electrochemical methods. Among these, AC impedance has been quoted to provide an upper estimate of the corrosion rate although the Tafel parameters relating corrosion rate and polarisation resistance need to be first evaluated (Williams and Asher, 1984). However, Electrochemical Impedance Spectroscopy (EIS) offers the advantage of providing enough insight on the formation and protection mechanisms of a given surface layer (Zeller and Savinella, 1986). Using the EIS method, various sacrificial Zn-based coatings have been evaluated because of their industrial application. For instance, Deslouis *et al*. (1989) determined the kinetics of corrosion of zinc in aerated Na_2SO_4 solutions and described a dissolution model. Corrosion was shown to occur essentially at the base of the pores of the coatings and

Corresponding Author: [1]Y. Hamlaoui, Centre Universitaire de Souk-Ahras, BP 1553 Souk-Ahars 41000, Algérie

progress of anodic dissolution gave rise to 4 loops with decreasing frequency (Cachet *et al*., 1992). Indeed, the compactness of the corrosion products layer developed on zinc needs to be introduced to evaluate its barrier effect (Suzuki, 1985). Based on this, further insight on Zn dissolution in sulphate medium has been provided by Cachet *et al*. (2001) who described a reaction model in which 3 paths associated to 3 adsorbed intermediates (Zn_{ad}^{+}, Zn_{ad}^{2+} and $ZnOH_{ad}$) were identified depending on the initial surface condition. Furthermore, the typical preferred crystal orientation of the coatings did not have any significant influence on the corrosion behaviour contrary to what is normally observed in pure zinc (Park and Spuznar, 1998; Sere *et al*., 1999). A more detailed study has been conducted by Pérez *et al*. (2002) by combining accelerated tests in a weathering cyclic chamber (deionised water/UV-IR radiation) with EIS measurements to track the degradation steps of an uncoated galvanised steel and of three differently painted galvanised steel. The authors could model the different dissolution behaviours thereafter concluding that the paints acted as selective membranes to avoid CO_2 uptake. Most of these studies have been carried out in laboratory based coatings. The presence of chlorides or soluble complex as Zn^{+2}-$Cl^{-}$$OH^{-}$ in the defects could initiate the localised corrosion (Peulon and Lincot, 1998). Also, a difference of surface potential can initiate a selective corrosion (Amedeh *et al*., 2002). To the best of our knowledge, only Barranco *et al*. (2004, a b) have focused on the study of EIS as an analytical tool to continuously monitor the corrosion of various industrial coatings in a 3% wt NaCl medium. The authors have claimed that empirical values of the B constant in the Stern-Geary equation must be introduced because of the over or underestimations of the corrosion behaviour of pure Zn and of Zn-5%Al (Galfan) coatings compared to Zn-10%Fe (Galvanneal) respectively. All the studies quoted below were focused on coatings without imperfections and elaborated under laboratory conditions. With an aim of making the coating surface porous, samples underwent an attack by HCl at weak concentrations. The present work is therefore focused on EIS as a potential analytical tool. The protective efficiency of the coatings was investigated by potentiodinamic polarization, EIS measurements combined with scanning electron microscopy. To this end, various corrosive media have been employed, namely NaCl, NaOH and natural rain water.

MATERIALS AND METHODS

Sample preparation and coatings: The substrate is a non alloyed steel S235JR (nominal composition according to EN10025-2:2004: Fe-0.17C-00.641 Mn-0.040S-0.012N-0.55Cu, wt%) with appropriate Si (0.14-0.25 wt%) and P (<0.035wt%) contents to allow galvanisation. The electroplating coatings were obtained from an aereted cyanide-free bath containing between 7-8.5 g L^{-1} of Zn (zinc sulphate) and 125-135 g L^{-1} NaOH. The bath température is maintained at 23°C under 2 A dm^{-2} of curent density during 32 min.

Thereafter, the coatings were thoroughly rinsed de-ionised water, in ethanol and the de-ionised again and then dried in air.

Morphological characterisation and elemental composition of the coatings was carried out by Scanning Electron Microscopy (SEM) coupled to Energy Dispersive Spectrometry (EDS) in a Philips XL 20 apparatus at 20 kV.

Corrosion tests and experimental set up: Samples of 4×4×0.05 cm were cut from the galvanised plates and most of the surface was protected with an adhesive film to leave a 1 cm^2 surface in contact with the corrosive medium. All the corrosion tests were normally repeated two or three times, checking that they presented reasonable reproducibility.

The corrosion tests were carried out at 25°C by magnetic stirring the solutions to obtain a slight vortex of the electrolyte. The corrosive media consisted of 0.1, 0.5 and 1 M NaCl, of 1M NaOH and of natural rain water. This latter was collected in the trial site of DRA Annaba Algeria between 13 et 21/01/2004. The chemical composition is given in Table 1.

The electrochemical experimental set-up is composed of a classic three electrodes cell using a platinum grid as counter electrode and a Saturated Calomel Electrode (SCE) as the reference one, the coated samples being connected to the working electrode. The measurements have been carried out using a potentiostat/galvanostat EGG 273A coupled to a Frequency Response Analyser (FRA) EGG 1025. The impedance data were obtained at the corrosion potential (E_{cor}) between 100 kHz and 100 mHz at 10 mV as the applied sinusoidal perturbation. The Tafel polarisation curves were obtained at a scanning rate of 60mV/ min between±250mV compared to the corrosion potential (E_{cor}). The experiments were monitored using the software EGG M352 and Powersine.

RESULTS AND DISCUSSION

Coating morphology: Electrodeposition was carried out in alkaline bath without additives and in experimental conditions.

Table 1: Average concentration in mg L^{-1} of natural rain water

pH	Total hardness	Mineralization	Ca^{2+}	Na^{+}	K^{+}	SO_4^{2-}	Cl^{-}	NO_3^{-}
7.1	65.00	80.00	20.00	1.50	1.00	16.75	10.50	8.00

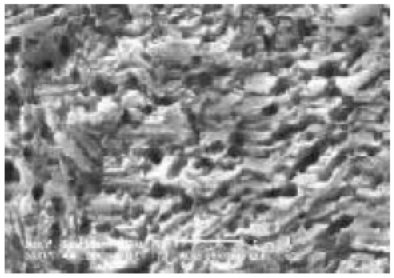

Fig. 1: SEM surface morphology of electroplated Zn coating

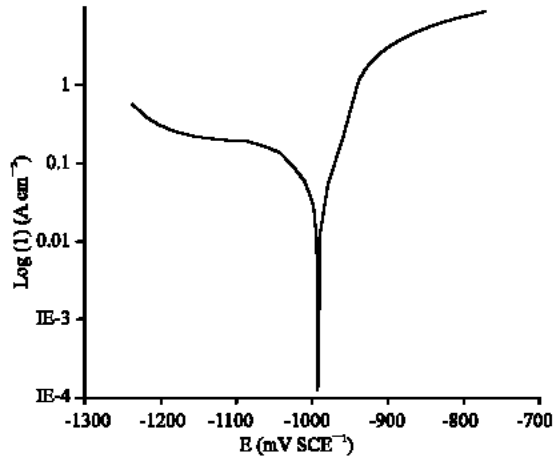

Fig. 2: Polarisation curve obtained on electroplated Zn coating in 0.1 M NaCi

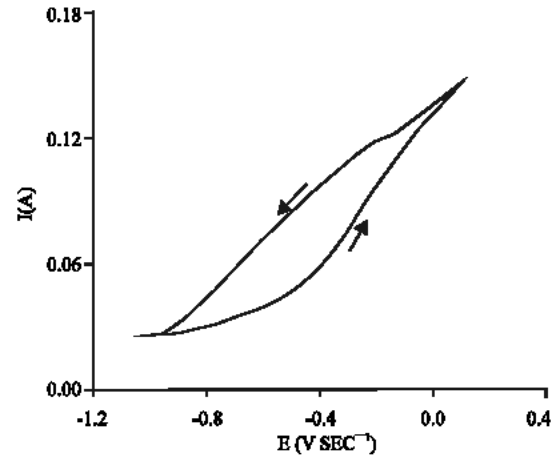

Fig. 3: Cyclic polarisation curve obtained on electroplytic coating in 0.1 M NCI

The coating obtained by electrodeposition was homogeneous adherent and without imperfection with a thickness of 10 μm. With an aim of creating imperfection and pores in the coating surface, our coating underwent an attack for few seconds by HCl at weak concentration 0.01M. For this purpose, the surface Fig. 1 shows a state of porosity on all surface.

Table 2: Electrochemical parameters obtained in NaCl solutions at different concentrations at room temperature of the Zn coatings

Medium	E_{corr} (mV SCE^{-1})	I_{corr} (μA cm^{-2})	V_{corr} (mm/an)
0.1 M	- 1020	99	1.47
0.5 M	-1016	117	1.74
1 M	- 944	170	2.53

Coating behavior in NaCl solution: In a first time, at least three DC polarisation tests have been carried out for each concentration. The results are gathered in Table 1. It can be easily observed that the corrosion rate in the aerated NaCl medium is under cathodic control (oxygen diffusion) (Fig. 2). Moreover, with the increase of the NaCl concentration, the corrosion potential is moved towards more anodic values. The increase of Icor and the decrease of Ecor could be explained by a corrosion processes developed under the oxide/hydroxide formed layer (at the interface substrate/film), since the porous nature of this layer(Cachet *et al*., 2002).

The cyclic polarisation curve obtained in 0.1M NaCl (Fig. 3) does not indicate any oxido-reduction peak with an important surface degradation.

In the Nyquist diagram the appearance of a semicircle at frequencies between 100 and 30 kHz is observed. Despite the change of the reference electrode, the modification of the distance between the electrodes and the conductivity of the electrolyte this feature continues to appear. Therefore, the shape of the cell is suspected to induce physical effects, as Zeller and Savinell (1986) also found in their studies on the AC impedance response of chromated electrogalvanised steel. Impedance diagrams Zn coatings at their corrosion potential have been obtained at different concentration of NaCl solution Table 2.

It can be observed in Table 3 that by increasing the NaCl concentration the charge transfer resistance decreases and therefore more corrosion occurs. Indeed, by increasing the NaCl concentration from 0.1 to 0.5 and 1 M, the transfer resistance loses 21 and 44% of its value respectively. On the contrary, the $R_{ct} \times I_{cor}$ product remain practically constant (20 mV). This results agreed rather well with the values of Icor calculated by extrapolation of Tafel slopes (Stern and Geary approximation). For this purpose, no correction is necessary. The double-layer capacity values do not seem to follow the trend of the resistance values, which lead us to believe that a

Table 3: Electrochemical impedance parameters obtained in NaCl solution at different concentrations and room temperature of electrolytic Zn coatings

Medium	R_{ct} (Ω)	f_{max}(Hz)	C_{dl} (μF)	α	R'(Ω)	F'$_{max}$ (Hz)	C'(F)
0.1M–pH solution 6.6	195	*127*	6.42	0.75	-58	0.3	-0.027
0.5M- pH solution 6.6	153	127	8.20	0.67	-10	0.3	-0.058
1 M-pH solution (6.7)	108	115	12.80	0.71	-18	9.0	-0.0009

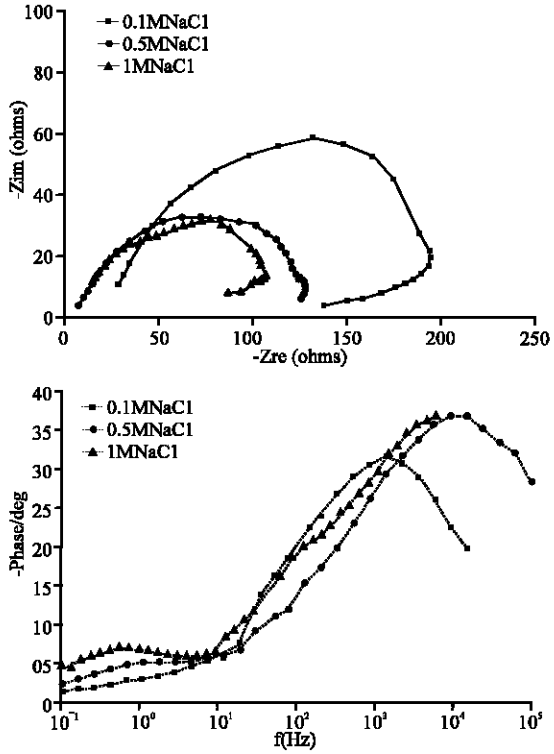

Fig. 4: EIS Nyquist a and bode b plots obtained in NaCI solution at different concentration, pH solution, pH solution and room temperature

dispersion of the relaxation time occurs. Ferreira *et al.* (2004) obtained two time constant for a HDG steel in 0.05M NaCl. The first one appear at intermediary frequencies followed by another at Low Frequency (LF). The latter was related to the oxide layer formed.

In our study the impedance diagram of the laboratory coatings obtained in a 0.1M NaCl solution shows two relaxation times (Fig. 4, Table 3). The first one corresponds to a capacitive loop HF, flattened and deformed in its left side, typical of a charge transfer whereas the second one is ascribed to an inductive loop in the capacitive plane. While passing to 0.5M the initiation of a new loop is observed with difficulty, this becomes clear at 1M. For this purpose, diagram will be composed of a capacitive loop between two inductive loops. In the literature, only one reactional model was proposed to describe the process of dissolution of pure Zn, that is in NaCl (Cachet *et al.*, 1992, 2001, 2002) or in Na_2SO_4 (Deslouis *et al.*, 1989).The model highlights two processes in parallel with the presence of two adsorbed

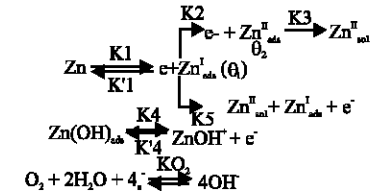

Fig. 5: Reaction scheme for zinc dissolution in aerated NaCI solution

Table 4: Electrochemical parameters obtained in 0.1M NaCl at different pH solutions at room temperature of the electrolytic Zn coatings

Medium	E_{corr} (mV/SCE)	I_{corr} (μA/cm^2)	V_{corr} (mm/an)
0.1 M-pH = 5	- 1010	101	1.51
0.1 M– pH = 6.6	- 1020	99	1.47
0.1 M-pH = 10	- 1015	118	0.27
0.1 M-pH = 11	- 1000	165	0.96

species (reaction pathway on Fig. 5). Thus, diagrams EIS comprise at LF three relaxation processes.

In the present study, the three relaxation processes are revealed only with concentration equals to 1M.

According to Cachet *et al.* (1992) the deformation of the left part of the capacitive loop HF is related to the existence of pores on the surface of the electrode. Moreover, the anodic reactions of dissolution do not appear only at their base i.e., their inner surface is regarded as inactive.

For this purpose, 4 relaxation processes observed in diagrams EIS can be allotted:

- The HF capacitive loop is related to the charge transfer.
- The HF inductive loop is related to the presence of Zn^I (intermediate species)
- The LF capacitive loop is related to the precipitation and migration of Zn^{II} by diffusion.
- The LF inductive loop is related to disappearance of oxide layer with time.

In order de see the influence of pH solution on the behavior and the applicability of the model, a series of tests were carried out in NaCl solution 0.1M at different pH (Table 4 and 5).

The variation of the solution pH between 5 and 10 seems affected neither the shape of the polarisation curves nor the corrosion currents densities. However, at pH 11 the corrosion process is accelerated (Fig. 6).

The low values of C_{dl} and the stability of the Rct values obtained at pH between (5-10) (Fig. 7) indicate the

Table 5: Electrochemical impedance parameters obtained in 0.1M NaCl at different pH solutions at room temperature of the electrolytic Zn coatings

Medium	R_{ct} (Ω)	f_{max}(Hz)	C_{dl} (μF)	α	R'(Ω)	F'_{max} (Hz)	C'(F)
0.1 M-pH = 5	180	127	7.00	0.78	-58	0.3	-0.027
0.1M–pH solution 6.6	195	*127*	6.42	0.75	-58	0.3	-0.027
0.1 M-pH= 10	179	204	4.00	0.79	-66	0.3	-0.024
0.1 M-pH = 11	142	127	9.00	0.85	-85	0.5	-0.019

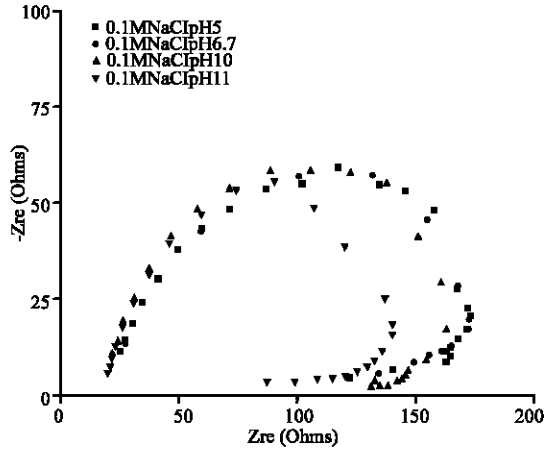

Fig. 6: EIS plots obtained on electroplated Zn coatings in 0.1M NaCl at different pH

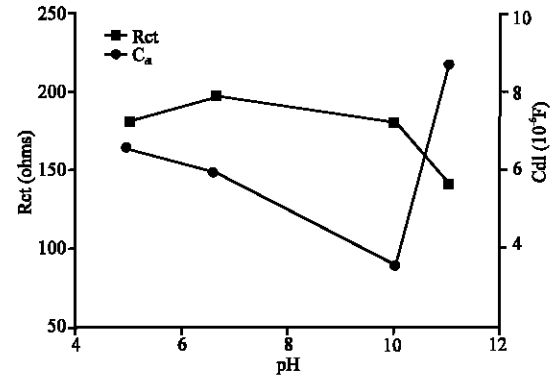

Fig. 7: Evolution of the time constants Rct and C_{dl} as function of pH of electroplared Zn coating

establishment of a chemical quasi-equilibrium of the corrosion products (temporary passivation) in agreement with the Pourbaix diagrams (Pourbaix, 1963). This layer starts to lose its stability at pH=11.

The EIS diagrams obtained at different pH showed the same bahavior (number of time relaxation) as that obtained at solution pH. For this purpose, we can conclude that the pH does not influence the mechanism of zinc dissolution. Then, the absence of the two relaxation processes in the diagrams obtained in NaCl 0.1M at different pH may be explained by:

The formation and transformation of the Zn^{I} species is fast and consequently it will occupy a weak surface

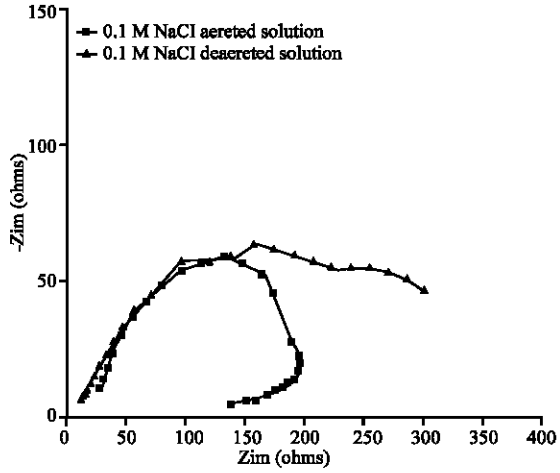

Fig. 8: EIS plots obtained on laboratory Zn coating in aerated and de-aerated NaCI 0.1M

coverage ((θ_1) is weak) and not at its lower chemical stability, thus the revelation of its relaxation process requires a frequential sweep lower than 0.1Hz.

The oxide/hydroxide layer formed on Zn is chemically stable (temporary passivation) what returns its speed of detachment weak and by consequently a braking of the fourth relaxation process. The weak appearance of an inductive loop LF in diagram EIS obtained in 0.5M confirms these assumptions.

The polarisation curves obtained at different NaCl concentrations showed clairly that the corrosion process is under cathodic control (oxygen reduction). Aiming to study the influence of oxygen, a test was carried out in 0,1M NaCl deaerated solution Fig. 8. The oxygen concentration, measured by standard oxymeter Z621 consort, in the aerated and deaerated solution is between 8 to 10 ppm and 1 to 2 ppm, respectively. Diagram EIS obtained in deaerated solutions present two capacitives loops overlapping. In the same way, Bode diagram, shows two very close time-constants. This behaviour can be explained by a fast filling of the pores by corrosion products made up of Zn hydroxide, which are converted into oxide according to:

$$Zn^{+2} + 2OH \longrightarrow Zn(OH)^{2} \longrightarrow ZnO + H^{2}O \quad (1)$$

In addition, the decrease in the quantity of oxygen in the medium slowed down the cathodic reaction (oxygen

Table 6: Electrochemical impedance parameters obtained in aerated and aerated 0.1M NaCl solution of the electrolytic Zn coatings

Medium	R_{ct} (Ω)	f_{max}(Hz)	C_{dl} (μF)	α	R'(Ω)	F'$_{max}$ (Hz)	C'(F)
0.1M-aerated	195	127	6.42	0.75	-58	0.3	-0.027
0.1M –deaerated	270	7	78.40	0.70	150	1.1	0.002

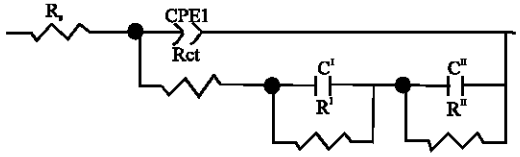

Fig. 9: Equivalent circuit reoresenting the interface Zinc coating/NaCI, NaOH and rainwater

reduction) and slightly decreases the pH on the surface of the electrode. With an aim to have an idea on the variation of the pH near the electrode in both cases of oxygenation, we suppose that only the cathodic reaction is oxygen reduction according to Eq. 1:

$$\text{At equlibriumstate}: = \frac{[O_2]_b\, nD_{O2}F}{\delta} = \frac{\left([OH^-]_s - [OH^-]_b\right)D_{OH^-}\ F}{\delta} \quad (2)$$

In this expression D_{O2} and D_{OH^-} are the diffusion coefficient of oxygen and hydroxide respectively. δ is the thickness of Nernst layer, $[O_2]_b$ and $[OH^-]_b$ are the concentrations of oxygen and hydroxide in bulk solution respectively, $[OH^-]_S$ is the concentration of hydroxide at surface electrode, F is the faraday number, n is the number of exchanged electrons (it can be 2 or 4). Because that the value of $[OH-]_b$ is very weak, we Considers that $[OH-]_b$ =0. Making the replacement in equation above, we obtain for n=2 a pH value of 10.35 and 11.28 for deaerated and aerated media respectively. According to the values illustrated in Table 4 and 6, we deduce that the coating in the deaerated solution (local pH =10.35) resists better against corrosion. Elimination of oxygen from the solution does seem to affect the shape of the curves and the resistance increases to 270Ω cm^{-2}. The oxygen reduction seems then dependent of the relaxation time and influences to overall current. The electrochemical parameters obtained from the stationary curves in a 0.1M NaCl solution seem to be in agreement with the results obtained from the frequency technique. At pH 9 and 10 the corrosion products are relatively stable and behave as a protective layer. Alcalinisation of the solution brings about dissolution of the corrosion products, which in turn increases the corrosion current.

Spectra obtained were simulated with equivalent circuit shown in Fig. 9. In this study, some parameters obtained by fiting the spectra using the Z view's ft engine program are interpreted. The circuit employed allows the identification of both solution Resistance (Rs) and charge transfer Resistance (Rct). It is important to mention that the double layer capacitance value is affected by imperfection of the surface and that this effect is simulated via a Constant Phase Element (CPE) with α represents a parameter describing the width of the material property distribution (dielectric times in frequency spaces). The different table obtained (Table 3-6) shows the representative parameter values of the best fit to experimental data and allow to describe the overall impedance through Eq. 3

$$Z(w) = R_S + \left[\frac{R_{ct}}{\left(jwC_{dl}R_{ct}\right)^{\alpha} + \frac{1}{1+\frac{Z_1+Z_2}{R_{ct}}}}\right] \quad (3)$$

$$\text{With } Z_1 = \frac{R'}{1+(jwC'R')^{\alpha_1}} \text{ and } Z_2 = \frac{R''}{1+(jwC''R'')^{\alpha_2}}$$

When the NaCl concentration is of 0.1M, then Z_2 = 0. On the other hand, for 1M, the parameters of the last inductive loop are: R'' =-32 ohms and C''=-0.02F at F = 0.233Hz.

Coating behavior in NaOH and rain water: Similarly to the studies carried out previously in NaCl, impedance diagrams at the corrosion potential have been studied in artificial rain water and NaOH 1M (Fig. 9). The obtained curves and results shown in Table 7 as expected show the adequate resistance of the laboratory coatings in both corroding media.

Indeed, the Rct value obtained in NaOH is seven times higher than that obtained in NaCl. On the other hand, the bode diagrams show only one time constant revealed between 10 et 1Hz. The same behavior was observed on hot deep galvanised steel (Ferreira *et al.*, 2004). This can be explained by the specifity, the nature and the stability of the formed corrosion products.

In NaOH, the expected corrosion product is mainly based on $Zn(OH)_2$ (Barranco *et al.*, 2004). In rain water hydrozincite $[Zn_5(CO_3)_2(OH)_6]$ has been shown to occur together with the already mentioned Zn corrosion products. The presence of this compound is known to result from direct reaction between Zn^{2+} and the carbonates (Sallivan and Worsley, 2002; Almeida *et al.*, 2000; Odnevall and Leygraf, 1993). However, in NaCl the

Table 7: Electrochemical impedance parameters of the electrolytic Zn coatings in different media at room temperature

Medium	Rct (Ω)	f_{max}(Hz)	C_{dl} (μF)	α	R'(Ω)	F'$_{max}$ (Hz)	C'(F)
1M NaCl	108	20.0	56	0.71	-18	9	-0.0009
1M NaOH	734	0.1	217	0.66	----	-----	-----
Rain water	138	204.0	56	0.77	-48	0.1	-0.0330

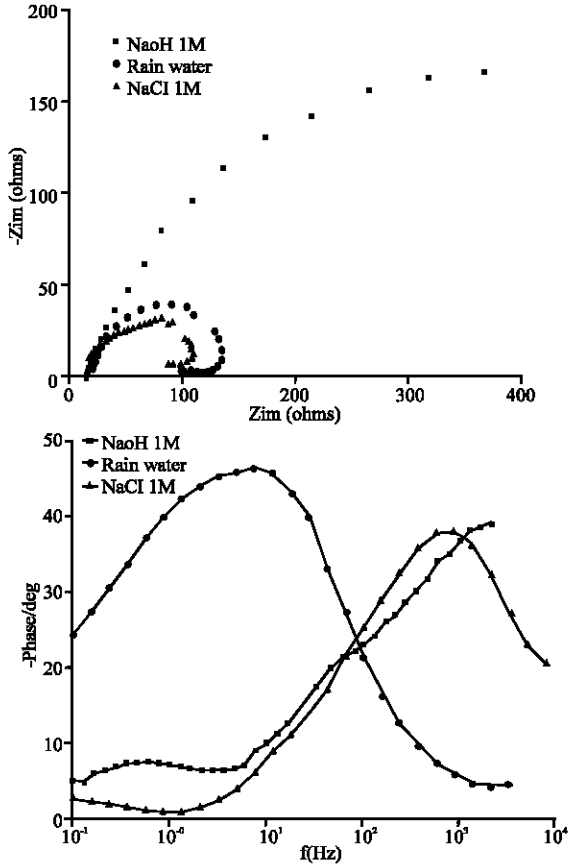

Fig. 10: EIS Nyquista a) and bode b) plots obtained on laboratory Zn coating in different media

products are to characterize by the presence of several compounds in particular: ZnO, $Zn(OH)_2$, Zn $5(OH)_8Cl_2.H_2O$ with the presence of several intermediate species such as $ZnOH^-$, ZnOH, $Zn(OH)^-_2$, $Zn(OH)_3^-$ (Cachet *et al*., 1992) Therefore, the impedance response of the laboratory Zn coating in either solution can be represented by the equivalent circuit already described in NaCl solution (Fig. 10).

To conclude, on laboratory coating, diagram obtained in NaCl 1M, shows three relaxation processes at LF, while at lower concentration and some is the pH of the medium, only one process is observed. Rct and Icor values obtained at pH between 5 to 10, are practically stable. In deaerated NaCl 0.1M, EIS diagram shows two time-constants at very close frequencies. Moreover, Rct increases by 30%. Moreover, EIS Diagrams indicate the porous character of the coating, whose dissolution mechanism appears at the base of the pores. While passing from 0.1 to 1M, Rct loses 44% of its value. This lets us to say that the pores observed on the coating surface are deep but they do not reach the surface of basic steel. In NaOH, Rct value obtained is seven times higher than those observed in 1M NaCl.

CONCLUSION

The characterization of the coating surface by MEB highlighted a state of apparent porosity but nondistinguishable between deep or only superficial. Deep Pores can blame the effectiveness of the coating against corrosion. Using EIS method coupled with other methods, we could shown that electrogalvanized samples presented a state of deep porosity but which do not reach basic steel.

According to the shape of the diagrams obtained, the pores are active in their base and inactive on their interior surface.

The reactional mechanism of dissolution of pure Zn in NaCl and Na_2SO_4 proposed by Delsouis and Cachet finds its application on steel galvanized only in NaCl ≥ 1M. on the other hand, at lower concentration, the diagrams of impedance obtained shows only one relaxation process BF.

The NaCl solution with weak concentration (<1M) does not constitute a likely medium to reveal (to initiate) the weakest processes and consequently to confirm the porous state of a EP steel.

The nucleation and initiation of slow reactions require a very low frequency sweep (lower than 100 mHz). Conversely, the low frequencies require long response times, which may modify the surface state of the electrode. The electrochemical impedance technique is therefore a very appropriate method to assess and understand the evolution of coatings as far as an adequate electrolyte is employed.

For this purpose, the NaCl 1M solution can allow to the controller quality to appreciate the surface quality of their coating and the information drawn from the diagrams obtained in the three mediums is complementary.

REFERENCES

Almeida, E., M. Morcillo and B. Rosales, 2000. Atmospheric corrosion of zinc Part 2: Marine atmospheres. Bri. Corr. J., 35: 289-296.

Amedeh, A., B. Pahlevani and S. Heshmati, 2002. Effects of rare earth metal addition on surface morphology and corrosion resistance of hot-dipped zinc coatings, Corr. Sci., 44: 2321-2331.

Barranco, V., S. Feliu Jr. and S. Feliu, 2004. EIS study of the corrosion behaviour of zinc-based coatings on steel in quiescent 3% NaCl solution. Part 1: Directly exposed coatings, Corr. Sci., 46: 2203-2220.

Barranco, V., S. Feliu Jr. and S. Feliu, 2004. EIS study of the corrosion behaviour of zinc-based coatings on steel in quiescent 3% NaCl solution. Part 2: Coatings covered with an inhibitor-containing lacquer, Corr. Sci., 46: 2221-2240.

Blanc, G., C. Gabrielli, M. Ksouri and R. Wiart, 1978. Experimental study of the relationships between the electrochemical noise and the structure of the electrodeposits of metals, Electrochem. Acta, 23: 337.

Cachet, C., F. Ganne, S. Joiret, G. Maurin, J. Petitjean, V. Vivier and R. Wiart, 2002. EIS investigation of zinc dissolution in aerated sulphate medium. Part II: zinc coatings Electrochem. Acta, 47: 3409-3422.

Cachet, C., B. Saidani and R. Wiart, 1992. The behavior of Zinc electrode in alkaline electrolytes: A kinetic analysis of anodic dissolution, J. Electrochem. Soc. 139 : 644-653.

Cachet, C., F. Ganne, G. Maurin, J. Petitjean, V. Vivier and R. Wiart, 2001. EIS investigation of zinc dissolution in aerated sulfate medium. Part I: Bulk zinc, Electrochem. Acta, 47: 509-518.

Deslouis, C., M. Duprat, Chr. Tournillon, 1989. The kinetics of zinc dissolution in aerated sodium sulphate solutions. A measurement of the corrosion rate by impedance techniques, Corr. Sci. 29: 13-30.

Ferreira, M.G.S., R.G. Duarte, M.F. Montemor and A.M.P. Simões, 2004. Silanes and rare earth salts as chromate replacers for pre-treatments on galvanised steel, Electroch. Acta, 49: 2927-2935.

Leroy, V., B. Schmitz, J. Metal, 1988. 17: 17.

Odnevall, I. and C. Leygraf, 1993. Formation of NaZn4Cl(OH)6SO4 • 6H2O in a marine atmosphere, Corr. Sci., 34: 1213-1229.

Park, H. and J.A. Spuznar, 1998. The role of texture and morphology in optimizing the corrosion resistance of zinc-based electrogalvanized coatings, Corr. Sci., 40: 525-545.

Pérez, C., A. Collazo, M. Izquierdo, P. Merino and X.R. Nóvoa, 2002. Comparative study between galvanised steel and three duplex systems submitted to a weathering cyclic test, Corr. Sci., 44: 481-500.

Peulon, S. and D. Lincot, 1998. Mechanistic study of cathodic electrodeposition of zinc oxide and zinc hydroxychloride films from oxygenated aqueous zinc chloride solutions, J. Electrochem. Soc., 145: 864.

Pourbaix, M., 1963. Atlas d'équilibres électrochimiques, Gauthier-Villars, Paris.

Sallivan, J.H. and D.A. Worsley, 2002. Zinc runoff fromgalvanised steel materials exposed in industrial/marine environment, Br. Corr. J., 37: 282-288.

Seré, P.R., J.D. Culcasi, C.I. Elsener and A.R. Di Sarli, 1999. The role of texture and morphology in optimizing the corrosion resistance of zinc-based electrogalvanized coatings Surf. Coatings Tech., 122: 143-149.

Suzuki, I., 1985. The behavior of corrosion products on zinc in sodium chloride solution Corr. Sci., 25: 1029-1034.

Williams, D.E. and J. Asher, 1984. Measurement of low corrosion rates: Comparison of A.C. impedance and thin layer activation methods, Corr. Sci., 24: 185-196.

Zeller, R.L., R.F. Savinelle, 1986. Interpretation of A.C. impedance response of chromated electrogalvanized steel, Corr. Sci., 26: 389-399.

Zhang, Z., W.H. Leng, Q.Y. Cai, F.H. Cao and J.Q. Zhang, 2005. Study of the zinc electroplating process using electrochemical noise technique, J. Elec. Anal. Chem., 578: 357-367.